International Journal of Pharmaceutics 419 (2011) 266–270

Contents lists available at ScienceDirect

International Journal of Pharmaceutics

journal homepage: www.elsevier.com/locate/ijpharm

Pharmaceutical Nanotechnology

OPA quantification of amino groups at the surface of Lipidic NanoCapsules (LNCs) for ligand coupling improvement

Thomas Perrier*, Florian Fouchet, Guillaume Bastiat, Patrick Saulnier, Jean-Pierre Benoît

INSERM U646, Ingénierie de la vectorisation particulaire, Bâtiment IRIS, niveau 3, rue des Capucins, 49933 Angers, France

ARTICLE INFO

Article history:
Received 22 March 2011
Received in revised form 15 July 2011
Accepted 18 July 2011
Available online 4 August 2011

Keywords:
Lipid Nanocapsules
Post-insertion
Amphiphilic phospholipids
Fluorescence

ABSTRACT

Lipidic NanoCapsules (LNCs) were prepared via an emulsion phase inversion method. Nanoparticles with hydrodynamic diameter of 25, 50 and 100 nm were easily obtained. Their surfaces are covered with short PEG chains (PEG 660) which are not bearing any chemical reactivities. Thus, in order to overcome this handicap towards post-functionalization possibilities, post-insertion of DSPE-PEG2000 amino (DSPA) can be employed. In order to characterize the insertion step, we have developed a chemical assay for the quantification of amino group inside the PEG shell of LNCs. Subsequently, the post-insertion yield was found to be comprised between 60 and 90% whatever the hydrodynamic diameter of the LNCs is. By means of simple calculations, the density of amino group is estimated to be closed to 0.2 and 1.2 molecules/nm^2. The formulation of LNCs and their controlled functionalization represent an interesting system for the development of bionanoconjugates in a short and effective process.

1. Introduction

The nanoparticle (NPs) family is composed by a broad range of nanoobjects as liposomes, vesicular carriers (nanocapsules, polymerosomes, niosomes), catanionic vesicles, polymer nanoparticles (nanospheres, solid lipid nanoparticles), micelles, dendrimers and hybrid organic/inorganic nanoparticles (magnetic nanoparticles, gold nanoparticles, quantum dots). All of these NPs have evoluted with time from first generation NPs, unable of targetability, to actual multifunctional nanoparticles (MFNPs).

Such nanoparticles are especially made to be used as nanomedecine (Riehemann et al., 2009) drug delivery vehicles, in particular for the treatment of diseases which are hardly cured such as cancers (Jabr-Milane et al., 2008; Davis et al., 2008) or infective pathologies as HIV. Indeed, NPs have been made to target cancer cells (McCarthy and Weissleder, 2008; Ganta et al., 2008; Cho et al., 2008) and to deliver drugs inside (Breunig et al., 2008) and/or in the close environment of the target such as tumors (Wagner, 2007; Nie et al., 2007). Anticancer drugs such as taxans or organometallic compounds have been used in both vitro/vivo experiments and were first investigated in order to answer to the urgent need for pharmaceutical forms with less counter side effects. In a second time, biomacromolecules (Sinha et al., 2006; Farokhzad et al., 2006) such as plasmids (Crystal, 1995; Meyer and Wagner, 2006; Donkuru et al., 2010), siRNA/shRNA (Elbashir et al., 2001; David et al., 2010) and proteins (Des Rieux et al., 2006) has been also investigated with promising results but also facing new challenges as these molecules are fragile both *in vitro* or *in vivo*. Furthermore, DNA based drugs need to reach the nucleus of the targeted cells, which means additional barriers to cross.

These obstacles reinforce the need of an engineered (Yih and Al-Fandi, 2006; Van Vlerken and Amiji, 2006) surface with responsive and biodegradable (Feng, 2004; Panyam and Labhasetwar, 2003) chemical bonds. All of these strategies (Allen and Cullis, 2004) imply the presence of ligands such as peptides (RGD, TAT), sugars (galactose) or proteins (growth factors, antibodies). Thus, RGD (Ruoslahti and Pierschbacher, 1987; Pasqualini et al., 1997) or TAT (Fawell et al., 1994; Vivès et al., 1997; Richard et al., 2003) possess great potentials towards targetability or enhancement of cell uptake; sugars as galactose (Morille et al., 2009) or mannose (Irache et al., 2008) has been used with success to target a whole organ (liver) or tumors, respectively. Regarding antibodies, they have been demonstrated to enhance targetability, leading to a new class of NPs, immunoNPs (Huwyler et al., 1996; Torchilin, 2006).

The introduction of these ligands involves a coupling between these ligands and NPs presenting reactive chemical groups such as primary amine, carboxylic acids, alkenes, azide/alkyne. In fact, numerous strategies (Perrier et al., 2010a,b) are available such as the well known carbodiimides chemistry (amines/carboxylic acids to form amide bonds) but also more recent developments like metathesis between alkene groups or reactions derived from the click chemistry school as copper catalyzed azide-alkyne cycloaddition (CuAAC) or thiol-ene chemistry. Hence, it is very important to quantify the amount of reactive entities with the best sensibility

* Corresponding author.
E-mail address: thomas.perrier2@hotmail.fr (T. Perrier).

0378-5173/$ – see front matter © 2011 Elsevier B.V. All rights reserved.
doi:10.1016/j.ijpharm.2011.07.028

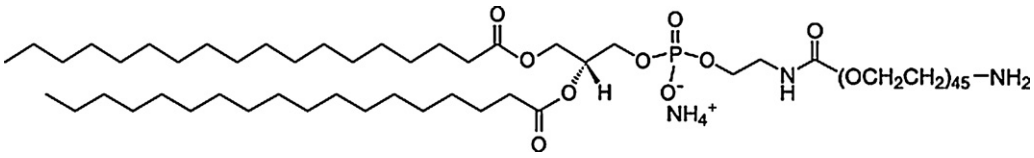

Fig. 1. Molecular structure of DSPA.

whatever the NPs are. It is as much important to set up methods suitable for the quantification of the ligands itself. This last point is emphasized by the fact that ligands are often present in the nanomolar range or less.

Our main objective is to develop a method for the quantification of reactive groups once purification step have been carried out. This information is highly relevant for the assessment of the yield of either formulation or post-formulation processes. It is also the central point in the establishment of a relationship between the density of reactive groups and/or ligands and expected biological activities.

The assay we have developed relies on a fluorescence quantification after a straightforward labeling step. The feasibility of fluorescence labeling of primary amino groups at the surface of NPs has been made for organic/inorganic NPs. However, these systems are different from LNCs used in this study. Indeed, LNCs are made of triglycerides and pegylated surfactants with a low amount of phospholipids unlike liposomes which are composed mainly of phospholipids. In this article, we present the setting up of an assay for the quantification of primary amino groups inside the shell of LNCs. The interface of LNCs has been modified by the post-insertion process (Perrier et al., 2010a,b) carried out with pegylated amphiphilic phospholipids, DSPE-PEG. This assay allowed us to determine the number of amino groups onto the LNCs surface after all the steps of the process, leading to the establishment of the post-insertion yields. All the more post-insertion has been widely used on liposomes or LNCs without the ability to characterize the amount of inserted molecules during the process. This assay is based on the o-phtalaldehyde (OPA) which is highly reactive towards amino groups and subsequently leads to fluorescent indole derivatives following Fig. 2. In spite of OPA is commonly used to label molecules after HPLC column with fluorescence based detection, it has not been used in the quantification of the structural components of NPs, in particular at the interface between NPs and external medium. However, this methodology has been used to assay gentamycin encapsulation yields inside liposomes (Gubernator et al., 2006).

2. Experimental

2.1. Materials

Labrafac® WL 1349 (Gattefossé S.A., Saint-Priest, France) is a mixture of capric and caprylic acid triglycerides. NaCl was purchased from Prolabo (Fontenay-sous-Bois, France) and water was obtained from a Milli-Q-plus® system (Millipore, Paris, France). Lipoïd® S75-3 (Lipoïd GmbH, Ludwigshafen, Germany) is a soybean lecithin made of 69% of phosphatidylcholine, 10% phosphatidylethanolamine and other phospholipids, and Solutol® HS 15 (BASF, Ludwigshafen, Germany) is a mixture of free polyethylene glycol 660 (PEG) and polyethylene glycol 660 hydroxystearate, corresponding to 13 units of PEG. The dialysis membrane was purchased from Spectrapore and has a molecular weight cut-off point equal to 100,000 Da.

1,2-Distearoyl-*sn*-glycero-3-phosphoethanolamine-*N*-[amino(polyethylene-glycol$_{2000}$)] (DSPA) (see Fig. 1), corresponding to 45 units of PEG, were supplied by Avanti® Polar Lipids Inc. (Alabaster, USA). o-Phtalaldehyde (OPA) was purchased from ThermoFischer and used as received.

2.2. Preparation of LNCs

This formulation method has already been well documented (Heurtault et al., 2002a, b) and can be briefly presented as follows: all components (Solutol HS-15, Lipoïd S75-3, sodium chloride, Labrafac CC and water) are mixed under magnetic stirring at an agitation speed of 200 rpm at room temperature leading to an O/W emulsion. After progressive heating at a 4 °C/min rate, a short interval of transparency at temperatures close to 70 °C can be observed, and the inverted phase (water droplets in oil) is obtained at 85 °C. At least three temperature cycles alternating from 60 to 85 °C at the same rate are applied near the phase-inversion zone. Thereafter, the mixture undergoes a fast cooling–dilution process: it is diluted 1:3.5 with 12.5 ml of cold water at 4 °C and stirred for 30 min., leading to the formation an LNC suspension of the desired size. LNCs are liquid core nanocapsules made of medium-chain triglycerides (Labrafac CC) surrounded by a surfactant shell assembled in a mixed monolayer of Solutol HS-15 and Lipoïd S75-3. The obtained size distribution depends on the relative amount of surfactants and oily phase i.e. triglycerides as described in Table 1.

2.3. Preparation of post-inserted LNCs

Post-inserted LNCs were prepared using the post-insertion technology previously developed on liposomes and adapted for the LNCs system by our group. The process is the incubation of DSPE-PEG micelles with LNCs and a molecular transfer of DSPE-PEG molecules from micelles to LNCs occurred. We have demonstrated that the preparation of post-inserted LNCs with DSPE-PEG bearing PEG moieties from 750 to 5000 g/mol. In each case, stable LNCs with narrow size distribution and specific electrokinetic properties are obtained (Perrier et al., 2010a,b).

In this article, the post-insertion is used for the preparation of LNCs with chemical reactive surface, ideally designed for the grafting of ligands. To a suspension of LNCs (1.75 ml) was added 1.30 ml of DSPA micelles in MilliQ water with a variable DSPA concentration. This concentration is expressed in % of the amount of surfactants employed in the formulation step. The post-insertion was performed during 105 min at 60 °C under continuous magnetic stirring. The reaction was stopped in an ice bath for 1 min. LNCs suspension were either used for the OPA quantification or were dialyzed against MilliQ water (4 l MilliQ water for 3 ml of LNCs

Table 1
Amount of excipients for the preparation of Lipidic NanoCapsules.

Excipients	20 nm LNCs	50 nm LNCs	100 nm LNCs
SolutolHS15®(g)	1.930	0.846	0.484
Lip old 75-3® (g)	0.075	0.075	0.075
NaCl (g)	0.089	0.089	0.089
Labrafac® (g)	0.846	1.028	1.209
Water (g)	2.055	2.962	3.143
Water 4 °C (g)	12.5	12.5	12.5
Total volume (ml)	17.5	17.5	17.5
Concentration (g/l)	168	115	104

Table 2
Hydrodynamic diameters and zeta potentials for LNCs.

Sample	HD (nm)	Pdl	Zeta potential (mV)
20 nmLNCs	23.9 ± 7.0	0.08	−17.1 ± 10.1
50 nmLNCs	49.2 ± 11.4	0.04	−8.25 ± 14.2
l00 nmLNCs	93.0 °C ± 26.8	0.05	−7.0 ± 12.2

suspension) for 24 h using a Spectra/Por dialysis bag with MWCO of 100,000 g/mol and then stored at 4 °C.

2.4. Calibration curve for OPA quantification assay

DSPA solutions were prepared by weighting DSPA powder into a scintillation vial. Each vial was placed into a water bath at 65 °C under magnetic stirring to ensure complete dissolution until a clear solution was obtained. Samples with concentrations up to 700 μg/ml were prepared. After cooling down, 30 μl of each DSPA solution were placed in a 96 wells-plate and 300 μl of OPA were added. The reaction medium was incubated at 25 °C for 5 min under a gentle shaking. Fluorescence was read with a fluoroskan at a 460 nm wavelength. After the substraction of the blank (MilliQ water), the calibration curve was drawn.

2.5. Quantification of DSPA by OPA assay

10 μl of post-inserted LNCs dialyzed or not, were placed in a black 96-well plate. 300 μl of OPA stock solution were added to each well and fluorescence was recorded with a fluoroskan (Thermo Scientific) with an excitation wavelength of 355 nm and an emission wavelength of 460 nm.

2.6. LNCs size distribution and zeta potentials

All particles sizes were measured by dynamic light scattering (DLS). The DLS instrument was a NanoZS (Malvern Instruments).

Measurements were performed at a 90° angle after dispersion of 50 μl of the LNCs suspension in 2.95 ml of MilliQ water. Each measurement was divided into 3 runs; each run consisting into 10 sub runs for a total of 30 laser light scattering acquisitions. The obtained time correlation functions were analyzed by autocorrelation using the method of cumulants.

3. Results

Three kinds of LNCs were produced directly in phosphate buffer saline (PBS) pH 7,4 with hydrodynamic diameter of 25, 50 and 93 nm. The formulation was based on a phase inversion process using an established experimental protocol (Heurtault et al., 2003). For each formulation, narrow size distribution were obtained as the polydispersity index was lower than 0.1. Zeta potentials were negative and are consistent with the pegylated surface of LNCs. Physico-chemical parameters of LNCs are reported in Table 2.

Post-inserted LNCs were then prepared using an established protocol. In each case, post-insertion process produced LNCs with a higher HD, as this later increase of 4–7 nm, respectively for 23 nm and 93 nm LNCs. These values are in accordance with previously published data and are typical for DSPE amphiphiles with a hydrophilic PEG2000 moiety. In all cases, PDI remains under 0.1 and zeta potentials became positives as presented in Table 3.

Zeta potentials values are comprised between 0 and +12.5 mV in accordance with the chemical nature of LNCs surface.

We first focused on the experimental conditions such as the ratio between both reactants, OPA and DSPA respectively. By monitoring the fluorescence intensity versus the OPA volume, it appeared that 300 μl of commercial OPA reagent solution was perfectly suited for 10 μl of DSPA solution at a concentration of 0.7 mg/ml. At the same time, we measured the fluorescence intensity as a function of time in order to evaluate the kinetic of the reaction between OPA and DSPA molecules (results not shown). It appeared that the fluorescence intensity was constant after 5 min of reaction at room temperature. Thus, these experimental conditions were chosen for the quantification experiments on LNC samples. By the way, the first problem was the signal due to auto fluorescence coming from LNC samples. We prepared standard suspension of LNCs with concentrations up to 168 g/L (expressed in organic mass). For each type of LNCs (25, 50 and 100 nm), measurements were done in triplicate and results are presented in Fig. 3.

Table 3
Hydrodynamic diameters and zeta potentials for post-inserted LNCs.

	HD(nm)	Pdl	Zeta potential (mV)
20 nmLXCs-5%DSPA	26.4 ± 7.4	0.06	−0.02 ± 21.1
20 nmLNCs-10%DSPA	27.6 ± 8.0	0.07	0.99 ± 17.7
20 nmLNCs-15%DSPA	27.0 ± 9.0	0.1	3.72 ± 15.4
50 nmLNCs-5%DSPA	53 2 ± 14.0	0.05	1.87 ± 10.9
50 nmLNCs-10%D8PA	53.3 ± 14.9	0.06	3.98 ± 7.2
50 nmLXCs-15%DSPA	53.8 ± 14.7	0.04	6.56 ± 8.3
100 nmLNCs-5%DSPA	101.9 ± 34.5	0.07	4.62 ± 9.2
100 nmLXCs-10%DSPA	100.9 ± 28.4	0.04	7.49 ± 9.9
100 nmLXCs + 15%DSPA	100.8 ± 29.S	0.04	9.44 ± 7.4
100 nmLNCs20%DSPA	102.5 ± 27.8	0.03	11.6 ± 12.7
100 nmLNCs-25%DSPA	101.4 ± 29.0	0.04	12.5 ± 10.9

The signal due to fluorescence of LNCs depends on the concentration following a linear relationship in all cases ($R^2 > 0.97$). We noticed that hydrodynamic size of particles plays a role in this noise signal as bigger the particles are higher the noise signal is. We have found that this size effect is a linear function (data not shown). Obviously, LNC samples should be diluted before OPA measurements in order to cancel out this noise signal.

To check the ability of OPA to react with DSPA, we performed assays onto calibrated DSPA samples and fluorescence was monitored. We found that OPA react with DSPA in both micellar and non-micellar solutions as critical micellar concentrations (CMC) of DSPA in closed to 1 μM. Thus we decided to built a calibration test and calibration curve could be drawn as shown in Fig. 4. OPA, after reaction with DSPA, gives fluorescent indole derivatives and the fluorescence was a linear function for DSPA concentration for concentration ranging from 0 to 700 μg/ml with excellent fitting parameters ($R^2 = 0.995$).

In order to quantify the amount of DSPA in each post-inserted LNCs sample, OPA assay was performed after the post-insertion step. By the way, we choose to dilute LNC samples 15, 20 and 25 times with PBS or MilliQ water before OPA assay. First of all, to assess the chemical reactivity of OPA towards DSPA in presence of LNCs, OPA assays were performed just after the post-insertion step. In all cases, DSPA concentrations were found to be closed to the maximum theoretical ones corresponding to the initial amount

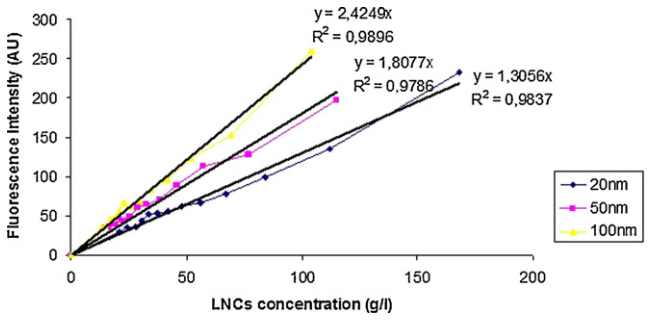

Fig. 3. Noise signal of LNC fluorescence as a function of LNC concentration.

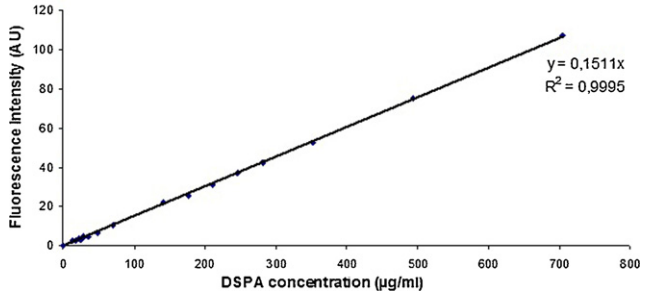

Fig. 4. Calibration curve for DSPA quantification by OPA.

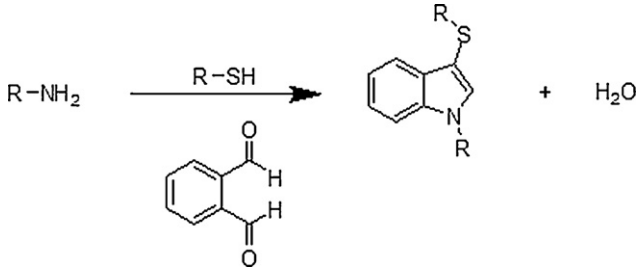

Fig. 2. Chemical equation for primary amines detection by OPA.

of added DSPA, confirming that the reaction was totally displaced to the formation of fluorescent indole derivatives. In order to remove the putative excess of DSPA, each LNCs sample was dialyzed against PBS until no variation of OPA fluorescence could be observed. Thus, an OPA assay was then done in order to quantify the remaining inserted DSPA. As DSPA amount can be quantified into LNC samples before and after dialysis, one can calculate the effective yield of post-insertion as described by Eq. (1). The post-insertion yield is comprised between 54 and 91% and is presented in Table 4.

$$R = \frac{\left(\mathrm{IF460_{sample}}\right) - \left(\mathrm{IF460_{blank}}\right)}{[\mathrm{DSPA}]_{\mathrm{theoritical}} \times D} \times F \times 100 \quad (1)$$

Where $\mathrm{IF460_{sample}}$ is the fluorescence intensity of test sample at 460 nm. $\mathrm{IF460_{blank}}$ is the fluorescence intensity of reference sample at 460 nm. $[\mathrm{DSPA}]_{\mathrm{theoretical}}$ is the concentration of DSPA inside the LNC samples in mg/ml. F is the dilution factor used in the preparation of test sample. D is the coefficient of the calibration curve. R is the post-insertion yield in percentage.

4. Discussion

We have demonstrated that we can produce LNCs on which amino groups are presented by means of the post-insertion process. Using an established protocol, LNCs are produced without altering the physico-chemical parameters of the original formulation, keeping the polydispersity index below 0.2. On the basis of previous work (Perrier et al., 2010a,b), DSPA molecules are transferred from DSPA micelles and inserted inside the LNCs shell. Zeta potential measurements confirm that these amino groups are located on the external layer of the ions-accessible layer of the polyethylene oxide (PEG) shell and thus, post-inserted LNCs present positive zeta potentials. This accessibility of amino groups was a good starting point with regards to the putative accessibility of amino groups to OPA. Preliminary studies on DSPA micelles indicate that OPA is able to react with primary amines even on the surface of a nano-object. The reaction is complete and fast under the experimental conditions i.e. room temperature and pH above 9. Effectively, at this pH and in the presence of a mercaptan such as ethanethiol; primary amines are nucleophilic and readily react with o-phtalaldehyde to form fluorescent 1-alkyl-2-alkylthio substituted isoindoles. By the way, OPA react with amino groups on the surface of LNCs and this assay allows us to quantify DSPA inside LNCs suspension. According to Fig. 2, LNCs produce a noise signal as LNCs are auto-fluorescent on the considered excitation/emission wavelengths. We evaluated that this noise signal is not significant if the concentration of LNCs is lower than 10 mg/ml, corresponding to 20 times dilution. Thus, we performed DSPA quantification on diluted LNC samples and succeeded to assess DSPA concentrations in the range of 67–671 μM. Thus, the OPA assay allows the quantification of DSPA in most of the LNC samples before their use in *in vitro/in vivo* experiments where LNCs should be diluted to higher fold. OPA assay permit to quantify DSPA after post-insertion and dialysis steps. According to Eq. (1), post-insertion yields depend on the hydrodynamic size of LNCs and on the starting amount of DSPA micelles. In each case, an optimum experiment prevails: around 10% for 20 and 50 nm LNCs; closed to 20% for 100 nm LNCs. As DSPA final concentration increases with the amount of DSPA micelles, the density of DSPA molecules at the surface also increases. As hydrodynamic size does not evolved with DSPA amount and zeta potentials still increase, we can affirm that post-insertion is a molecular insertion of DSPA inside the LNC shell. This result is in total accordance with previous published data (Perrier et al., 2010a,b) and OPA confirms this hypothesis. Furthermore, we have calculated the average molecular area (for Solutol, Lipoïd and DSPA molecules) at the LNC surface and post-insertion does not lead to a compression of molecules at the oil/water interface. Average molecular area are presented in Table 5 and are in agreement with published characteristics for surfactants at oil/water interface or for phospholipids organized in bilayer membranes.

OPA assay enables to calculate the density of amino groups on the LNCs surface. Results of calculations are presented in Table 6.

Table 4
Post-insertion yield for each post-insertion experimental condition.

	Post-insertion yield in %
20 nm LNCs	
5% DSPE PEG NH2	54.5
10% DSPE PEG NH2	76.5
15% DSPE PEG NH2	66 5
50 nm LNCs	
5% DSPE PEG NH2	66.3
10% DSPE PEG NH2	78.3
15% DSFE PEGNH2	76.5
100 nm LNCs	
5% DSPE PEG NH2	63.5
10% DSPE PEG NH2	74.1
15% DSPE PEG NH2	72.9
20% DSPE PEG NH2	91.8
25% DSFE PEGNH2	75.5

Table 5
Average molecular area on the surface of LNCs before and after post-insertion.

	Before post-insertion Interfacial average molecular area nm²	After post-insertion Interfacial average molecular area nm²
20 mn LNCs + 5% DSPA	0.18	0.17
20 nm LNCs + 10% DSPA	0.18	0.16
2Onm LNCs + 15% DSPA	0.18	0.15
50 nm LNCs + 5% DSPA	0.24	0.23
50 nm LNCs + 10% DSPA	0.24	0.21
50 nm LNCs + 15% DSPA	0.24	0.20
100 nm LNCs + 5% DSPA	0.25	0.24
100 nm LNCs + 10% DSPA	0.25	0.22
100 nm LNCs + I5% DSPA	0.25	0.21
100 nm LNCs + 20% DSPA	0.25	0.19
100 nm LNCs + 25% DSPA	0.25	0.19

Table 6
DSPA molecular density on the surface of LNCs for each post-insertion condition.

	DSPA molecules/LNC	DSPA molecules/nm^2
20 nm LNCs + 5% DSPA	476	0.2
20 nm LNCs + 10% DSPA	1525	0.6
20 nm LNCs + 15% DSPA	1833	0.8
50 nm LNCs + 5% DSPA	1904	0.2
50 nm LNCs + 10% DSPA	4554	0.5
50 nm LNCs + 15% DSPA	6711	0.8
100 nml LNCs + 5%DSPA	6527	0.2
100 nml LNCs + 10%DSPA	15,229	0.5
100 nml LNCs + 15%DSPA	22,480	0.7
100 nml LNCs + 20%DSPA	37,709	1.2
100 nml LNCs + 25%DSPA	38,797	1.2

Fundamental differences appear in terms of DSPA density; depending on both the size pf LNCS and on the amount of DSPA used for post-insertion. The density of DSPA increases with both DSPA amount and LNCs hydrodynamic size. We can comment that post-insertion can produce radically different LNCs in terms of functionality. Considering the amino groups are often used for chemical engineering, the ligand density can trigger off the bioactivity of the MFNPs after *in vitro* or *in vivo* administration. Indeed, the density of ligand such as peptides (Fawell et al., 1994; Vivès et al., 1997; Richard et al., 2003), antibodies (Huwyler et al., 1996; Torchilin, 2006), proteins (Ruoslahti and Pierschbacher, 1987; Pasqualini et al., 1997), sugars (Irache et al., 2008; Morille et al., 2009), is the basis for the control of bioactivity from biological (Huskens et al., 2004; Hong et al., 2007) and chemical (Mammen et al., 1998; Kitov and Bundle, 2003) point of view. In this way, OPA assay is the basement of a strategy aimed to develop precise nanoparticle bionanoconjugates and to control the targeting properties of such multifunctional NPs.

5. Conclusion

We have adapted a fluorescent assay based on OPA that allows the quantification of DSPA molecules inserted inside the LNCs by means of post-insertion. We have shown that this quantification could be routinely used on LNC samples. This assay permits to confirm the molecular insertion of DSPA inside the LNCs shell during post-insertion. OPA quantification is a straightforward strategy to develop controlled MFNPs suitable for targeting and therapeutic purposes. OPA could also be used to quantify other biomolecules and this work will be the scope of another article.

Acknowledgments

We wish to thank European Union (Project Nanoear) and the Région Pays de la Loire for providing financial support for this work.

References

Allen, T.M., Cullis, P.R., 2004. Drug delivery systems: entering the mainstream. Science 303, 1818–1822.
Breunig, M., Bauer, S., Goepferich, A., 2008. Polymers and nanoparticles: intelligent tools for intracellular targeting? Eur. J. Pharm. Biopharm. 68, 112–128.
Cho, K., Wang, X., Nie, S., Chen, Z., Shin, D.M., 2008. Therapeutic nanoparticles for drug delivery in cancer. Clin. Cancer Res. 14, 1310–1316.
Crystal, R.G., 1995. Transfer of genes to humans: early lessons and obstacles to success. Science 270, 404–410.
David, S., Pitard, B., Benoît, J.-P., Passirani, C., 2010. Non-viral nanosystems for systemic siRNA delivery. Pharmacol. Res. 62, 100–114.
Davis, M.E., Chen, Z., Shin, D.M., 2008. Nanoparticle therapeutics: an emerging treatment modality for cancer. Nat. Rev. Drug Discov. 7, 771–782.
Des Rieux, A., Fievez, V., Garinot, M., Schneider, Y.-J., Préat, V., 2006. Nanoparticles as potential oral delivery systems of proteins and vaccines: a mechanistic approach. J. Control. Release 116, 1–27.
Donkuru, M., Badea, I., Wettig, S., Verrall, R., Elsabahy, M., Foldvari, M., 2010. Advancing nonviral gene delivery: lipid- and surfactant-based nanoparticle design strategies. Nanomedicine 5, 1103–1127.
Elbashir, S.M., Harborth, J., Lendeckel, W., Yalcin, A., Weber, K., Tuschl, T., 2001. Duplexes of 21-nucleotide RNAs mediate RNA interference in cultured mammalian cells. Nature 411, 494–498.
Farokhzad, O.C., Karp, J.M., Langer, R., 2006. Nanoparticle-aptamer bioconjugates for cancer targeting. Expert Opin. Drug Deliv. 3, 311–324.
Fawell, S., Seery, J., Daikh, Y., Moore, C., Chen, L.L., Pepinsky, B., Barsoum, J., 1994. Tat-mediated delivery of heterologous proteins into cells. PNAS 91, 664–668.
Feng, S.-S., 2004. Nanoparticles of biodegradable polymers for new-concept chemotherapy. Expert Rev. Med. Devices 1, 115–125.
Ganta, S., Devalapally, H., Shahiwala, A., Amiji, M., 2008. A review of stimuli-responsive nanocarriers for drug and gene delivery. J. Control. Release 126, 187–204.
Gubernator, J., Drulis-Kawa, Z., Kozubec, A., 2006. A simply and sensitive fluorometric method for determination of gentamycin in liposomal suspensions. Int. J. Pharm. 327, 104–109.
Heurtault, B., Saulnier, P., Pech, B., Proust, J.E., Benoît, J.P., 2002a. Properties of polyethylene glycol 660 12-hydroxy stearate at a triglyceride/water interface. Int. J. Pharm. 242, 167–170.
Heurtault, B., Saulnier, P., Pech, B., Proust, J.-E., Benoit, J.-P., 2002b. A novel phase inversion-based process for the preparation of lipid nanocarriers. Pharm. Res. 19, 875–880.
Heurtault, B., Saulnier, P., Pech, B., Venier-Julienne, M.-C., Proust, J.-E., Phan-Tan-Luu, R., Benoît, J.-P., 2003. The influence of lipid nanocapsule composition on their size distribution. Eur. J. Pharm. Sci. 18, 55–61.
Hong, S., Leroueil, P.R., Majoros, I.J., Orr, B.G., Baker Jr., J.R., Banaszak Holl, M.M., 2007. The binding avidity of a nanoparticle-based multivalent targeted drug delivery platform. Chem. Biol. 14, 107–115.
Huskens, J., Mulder, A., Auletta, T., Nijhuis, C.A., Ludden, M.J.W., Reinhoudt, D.N., 2004. A model for describing the thermodynamics of multivalent host–guest interactions at interfaces. J. Am. Chem. Soc. 126, 6784–6797.
Huwyler, J., Wu, D., Pardridge, W.M., 1996. Brain drug delivery of small molecules using immunoliposomes. PNAS 93, 14164–14169.
Irache, J.M., Salman, H.H., Gamazo, C., Espuelas, S., 2008. Mannose-targeted systems for the delivery of therapeutics. Expert Opin. Drug Deliv. 5, 703–724.
Jabr-Milane, L.S., van Vlerken, L.E., Yadav, S., Amiji, M.M., 2008. Multi-functional nanocarriers to overcome tumor drug resistance. Cancer Treatment Rev. 34, 592–602.
Kitov, P.I., Bundle, D.R., 2003. On the nature of the multivalency effect: a thermodynamic model. J. Am. Chem. Soc. 125, 16271–16284.
Mammen, M., Choi, S.-K., Whitesides, G.M., 1998. Polyvalent interactions in biological systems: implications for design and use of multivalent ligands and inhibitors. Angew. Chem. Int. Ed. 37, 2755–2794.
McCarthy, J.R., Weissleder, R., 2008. Multifunctional magnetic nanoparticles for targeted imaging and therapy. Adv. Drug Deliv. Rev. 60, 1241–1251.
Meyer, M., Wagner, E., 2006. Recent developments in the application of plasmid DNA-based vectors and small interfering RNA therapeutics for cancer. Hum. Genet. Ther. 17, 1062–1076.
Morille, M., Passirani, C., Letrou-Bonneval, E., Benoit, J.P., Pitard, B., 2009. Galactosylated DNA lipid nanocapsules for efficient hepatocyte targeting. Int. J. Pharm. 379, 293–300.
Nie, S., Xing, Y., Kim, G.J., Simons, J.W., 2007. Nanotechnology applications in cancer. Annu. Rev. Biomed. Eng. 9, 257–288.
Panyam, J., Labhasetwar, V., 2003. Biodegradable nanoparticles for drug and gene delivery to cells and tissue. Adv. Drug Deliv. Rev. 55, 329–347.
Pasqualini, R., Koivunen, E., Ruoslahti, E., 1997. αv integrins as receptors for tumor targeting by circulating ligands. Nature Biotechnol. 15, 542–546.
Perrier, T., Saulnier, P., Benoît, J.-P., 2010a. Methods for the functionalisation of nanoparticles: new insights and perspectives. Chem. A: Eur. J. 16, 11516–11529.
Perrier, T., Saulnier, P., Fouchet, F., Lautram, N., Benoît, J.P., 2010b. Post-insertion into Lipid NanoCapsules (LNCs): from experimental aspects to mechanisms. Int. J. Pharm. 396, 204–209.
Richard, J.P., Melikov, K., Vives, E., Ramos, C., Verbeure, B., Gait, M.J., Chernomordik, L.V., Lebleu, B., 2003. Cell-penetrating peptides: a reevaluation of the mechanism of cellular uptake. J. Biol. Chem. 278, 585–590.
Riehemann, K., Schneider, S.W., Luger, T.A., Godin, B., Ferrari, M., Fuchs, H., 2009. Nanomedicine – Challenge and perspectives. Angew. Chem. Int. Ed. 48, 872–897.
Ruoslahti, E., Pierschbacher, M.D., 1987. New perspectives in cell adhesion: RGD and integrins. Science 238, 491–497.
Sinha, R., Kim, G.J., Nie, S., Shin, D.M., 2006. Nanotechnology in cancer therapeutics: bioconjugated nanoparticles for drug delivery. Mol. Cancer Ther. 5, 1909–1917.
Torchilin, V.P., 2006. Multifunctional nanocarriers. Adv. Drug Deliv. Rev. 58, 1532–1555.
Van Vlerken, L.E., Amiji, M.M., 2006. Multi-functional polymeric nanoparticles for tumour-targeted drug delivery. Expert Opin. Drug Deliv. 3, 205–216.
Vivès, E., Brodin, P., Lebleu, B., 1997. A truncated HIV-1 Tat protein basic domain rapidly translocates through the plasma membrane and accumulates in the cell nucleus. J. Biol. Chem. 272, 16010–16017.
Wagner, E., 2007. Programmed drug delivery: nanosystems for tumor targeting. Expert Opin. Biol. Ther. 7, 587–593.
Yih, T.C., Al-Fandi, M., 2006. Engineered nanoparticles as precise drug delivery systems. J. Cell Biochem. 97, 1184–1190.